ISSN 0020-1685, Inorganic Materials, 2019, Vol. 55, No. 7, pp. 715–723. © Pleiades Publishing, Ltd., 2019.
Russian Text © The Author(s), 2019, published in Neorganicheskie Materialy, 2019, Vol. 55, No. 7, pp. 760–768.

Structure and Thermal Stability of Lithium-Substituted Hydroxyapatite Ceramics

V. V. Smirnov[a], *, S. M. Barinov[a], S. V. Smirnov[a], A. I. Krylov[a], O. S. Antonova[a], M. A. Goldberg[a], T. O. Obolkina[a], A. A. Konovalov[a], and A. V. Leonov[b]

[a] *Baikov Institute of Metallurgy and Materials Science, Russian Academy of Sciences, Leninskii pr. 49, Moscow, 119334 Russia*
[b] *Moscow State University, Moscow, 119991 Russia*
**e-mail: smirnov2007@mail.ru*

Received August 14, 2018; revised February 14, 2019; accepted February 18, 2019

Abstract—We have studied the effect of doping with lithium cations on the phase composition, lattice parameters, and crystallite size of hydroxyapatite at different heat treatment temperatures (900, 1200, and 1400°C). The results demonstrate that, at high degrees of substitution (20 mol %) and heat treatment temperatures of 1200 and 1400°C, lithium cations contribute to conversion of apatite into lithium-substituted tricalcium phosphate. At degrees of substitution of 1, 5, and 10 mol %, the addition of lithium causes no destabilization of the apatite structure even at a temperature of 1400°C.

Keywords: bioceramics, hydroxyapatite, phase composition, lattice parameters

DOI: 10.1134/S0020168519070185

INTRODUCTION

Hydroxyapatite (HA), $Ca_5(PO_4)_3(OH)$, is one of the most promising materials for use in regenerative and reconstructive surgery for injured bone tissue replacement. The reason for this is that HA is similar in mineralogical composition to natural bone tissue. HA materials are intended mainly for the fabrication of high-strength, nonresorbable implants, which should have excellent mechanical properties [1]. A topical issue is studies aimed at designing HA materials with controlled properties, for example, via modification with metal ions [2, 3]. A promising approach is to produce lithium-substituted (Li-HA) materials. This is due to the effect of lithium on the biological properties of HA: it raises the rate of osteogenic differentiation of mesenchymal stem cells [4]; accelerates HA degradation owing to the activation of cells involved in the bone tissue remodeling process [5]; and activates beta-catenin (signal mediator), thus contributing to bone healing [6]. The addition of lithium improves HA sinterability and, as a consequence, contributes to the strength of HA-based ceramic materials by reducing their porosity.

There is limited information about the properties of apatites containing lithium ions, especially as to the effect of lithium cations on their lattice parameters and the stability of their phase composition during heat treatment of HA materials in a wide temperature range. For example, Drdlik et al. [7] studied the phase composition and structure of ceramics up to 1250°C at lithium contents below 1%. Their results show that at 1050°C HA converts into β-tricalcium phosphate (TCP), whereas the major phase forming at 1250°C is α-TCP. According to studies at higher degrees of substitution (10 and 20 at %) [8], heat treatment at 900°C causes HA to completely convert into $Ca_{10}Li(PO_4)_7$. Badran et al. [9] described the preparation of Li-HA containing 0, 1, 5, 10, 20, and 40% lithium oxide. They determined the phase composition and lattice parameters of the synthesized materials. However, the heat treatment temperature in their study was relatively low, just 100°C, which prevented them from assessing the effect of lithium on the phase composition, thermal stability, and lattice parameters of materials with a high degree of crystallinity.

In this paper, we examine how the degree of substitution of lithium cations (0, 1, 5, 10, and 20 mol %) for calcium ions in HA ceramics influences the variation of their lattice parameters and phase composition with heat treatment temperature (900, 1200, and 1400°C). The choice of these temperatures was prompted by specific features of the technology of HA ceramics, which are commonly produced by sintering at temperatures from 1200 to 1300°C.

EXPERIMENTAL

The nominal compositions of the synthesized compounds are listed in Table 1. The samples were prepared by precipitation from aqueous solutions. To this end, ammonium hydrogen phosphate solutions

Table 1. Compositions of the materials

Notation	Degree of substitution, mol %	Nominal formula
0Li-HA	0	$Ca_{10}(PO_4)_6(OH)_2$
1Li-HA	1	$Ca_{9.9}Li_{0.2}(PO_4)_6(OH)_2$
5Li-HA	5	$Ca_{9.5}Li(PO_4)_6(OH)_2$
10Li-HA	10	$Ca_9Li_2(PO_4)_6(OH)_2$
20Li-HA	20	$Ca_8Li_4(PO_4)_6(OH)_2$

were added to a stirred solution containing calcium and lithium nitrates. Precipitation was carried out at pH 9.3–9.7. The amounts of chemicals were calculated for the reaction scheme

$$(10-x)Ca(NO_3)_2 + 6(NH_4)_2HPO_4 + 2xLiNO_3 \rightarrow Ca_{10-x}Li_{2x}(PO_4)_6(OH)_2, \quad (1)$$

where $x = 0$, 0.1, 0.5, 1.0, or 2.0.

After the synthesis, the precipitate was aged for 21 days to increase the degree of crystallinity of the apatite phase [10]. Next, the precipitate was filtered off. The resultant powders were calcined at 900, 1200, and 1400°C.

The materials were characterized by X-ray diffraction (Shimadzu XRD 6000 diffractometer) using the JCPDS PCPDFWIN database. Unit-cell parameters were determined by the Rietveld method using the FullProf Suite. IR spectra were measured on a Thermo Nicolet Avatar 330 Fourier transform IR spectrometer. Porosity of the samples was assessed by hydrostatic weighing in accordance with the Russian Federation State Standard GOST 2409-95. To this end, samples 30 × 4 × 4 mm in dimensions were pressed in a steel press die at a specific pressure of 100 MPa and then heat-treated in the temperature range 900–1400°C.

RESULTS AND DISCUSSION

After heat treatment at 900°C, the 0Li-HA materials consisted of one phase: HA. Further raising the temperature to 1200°C led to the formation of a small amount of β-TCP. These results are consistent with data reported by Meejoo et al. [11], which show that HA partially converts into β-TCP after heat treatment in the range 900–1200°C. Further raising the temperature to 1400°C led to the formation of up to 30% α-TCP. After heat treatment at 900°C, all of the Li-HA substituted materials consisted of only an apatite phase (Fig. 1). Note that the percentage of lithium had no effect on the degree of crystallinity of the samples (on the intensity of diffraction peaks). After heat treatment at 1200°C, the samples with a degree of substitution from 5 to 10 mol % were found to contain a small amount of β-TCP (Fig. 2). Note that the intensity of diffraction peaks decreases with increasing lithium content, which is due to the lower degree of crystallinity of the major phase. In the case of the 20Li-HA materials, the composition changes sharply, namely, the apatite decomposes into two phases: β-TCP (20%) and the lithium calcium phosphate $LiCaPO_4$ (LCP). Heat treatment at 1400°C led to the formation of the lithium-substituted compound $Ca_{10}Li(PO_4)_7$ (Li-TCP) (15%) starting at the composition 5Li-HA (Fig. 3). Further raising the percentage of lithium led to an increase in the amount of Li-TCP and a reduction in HA content (Table 2), which was accompanied by a decrease in α-TCP content from 27% (0Li-HA) to 3% (1Li-HA) and to zero in the lithium-rich materials (5Li-HA, 10Li-HA, and 20Li-HA). Li-TCP (JCPDS card no. 45-550) in the 5Li-HA, 10Li-HA, and 20Li-HA materials was difficult to identify because its diffraction peaks were close to those of β-TCP (JCPDS card no. 9-169).

We examined in detail the major peaks and found the reflections from Li-TCP to be shifted to larger angles on average by 0.2° relative to β-TCP. This was interpreted in accordance with the JCPDS Powder Diffraction File as evidence for the formation of a new lithium-containing compound, $Ca_{10}Li(PO_4)_7$, because substitution of a smaller cation (Li^+) for a larger cation (Ca^{2+}) is known to reduce the lattice parameters of the material [12, 13].

It should also be noted that heat treatment at 1200°C led to the formation of two phases in addition to HA: β-TCP (Ca_3PO_4) and LCP ($LiCaPO_4$), with a Ca/Li ratio of 50/50. At the same time, at a temperature of 1400°C only one compound was formed in addition to HA: $Ca_{10}Li(PO_4)_7$, with a Ca/Li ratio of 10/1. This effect can be accounted for in terms of the lithium redistribution between the phases present. At low heat treatment temperatures (1200°C), the process yields a mixture of phases differing in lithium content, which may be a consequence of the inhomogeneous component distribution produced in the course of the synthesis of the materials. As the temperature is raised (1400°C), diffusion processes become more active, resulting in a redistribution of lithium between the phases present and the formation of one lithium-substituted compound with low lithium content.

Moreover, $LiCaPO_4$ was reported to lose lithium at high temperatures [14]. This may lead to the formation

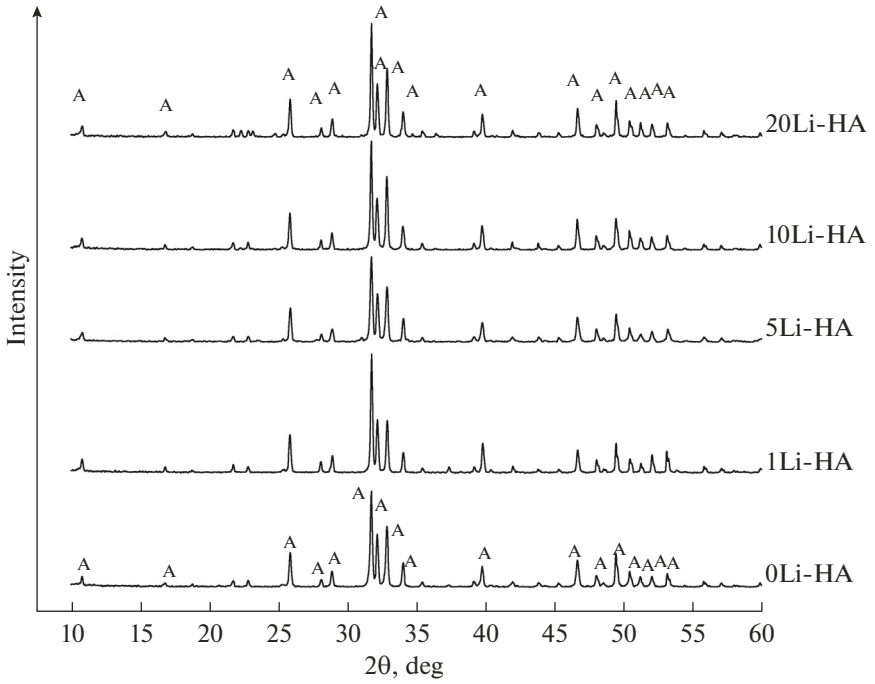

Fig. 1. X-ray diffraction patterns of the powders after heat treatment at 900°C (the letter A denotes HA).

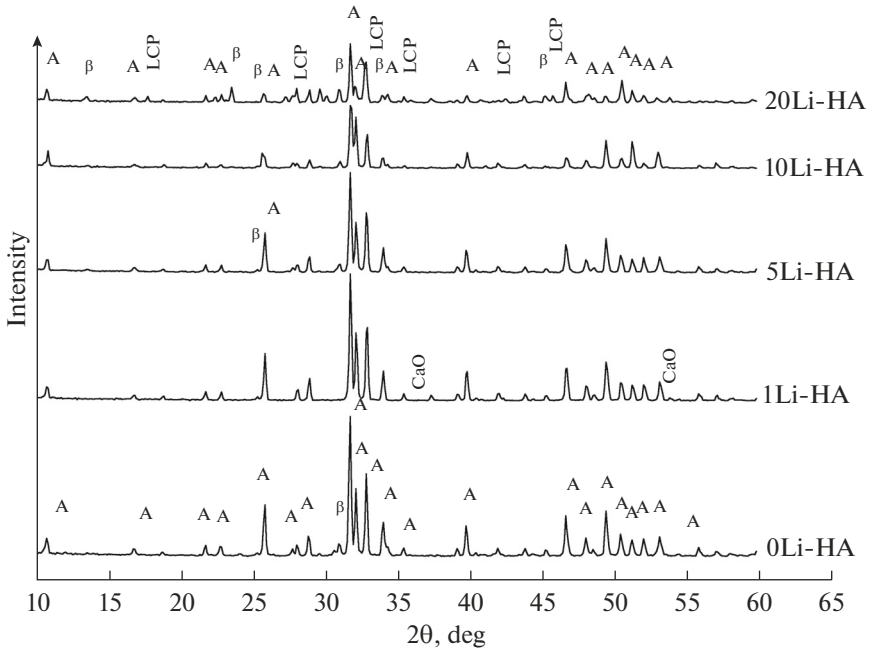

Fig. 2. X-ray diffraction patterns of the powders after heat treatment at 1200°C (the letter A denotes HA; β denotes β-TCP, and LCP denotes $LiCaPO_4$).

of compounds with the whitlockite structure, including $Ca_{10}Li(PO_4)_7$.

X-ray diffraction measurements showed that the peaks of the 1Li-HA material heat-treated at 900°C were shifted to smaller 2θ angles relative to pure HA. This points to an increase in lattice parameters (Table 3). This effect can be accounted for by the presence of lithium cations in interstices, which leads to the formation of an interstitial solid solution and vacancies in the cation sublattice. This appears to be the most likely

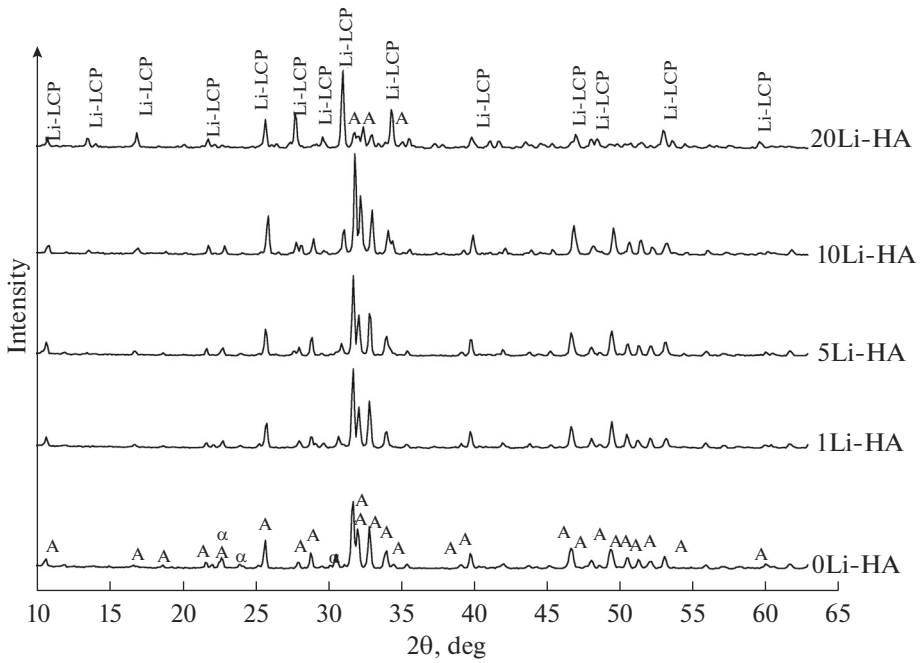

Fig. 3. X-ray diffraction patterns of the powders after heat treatment at 1400°C (the letter A denotes HA; α denotes α-TCP, and Li-TCP denotes $Ca_{10}Li(PO_4)_7$).

scenario, given that the ionic radius of Li is considerably smaller than that of Ca (Ca^{2+}, 1.04 Å; Li^+, 0.68 Å).

It should also be taken into account that the HA structure was formed only gradually, over 21 days of aging in mother liquor [10].

The aging process involves reactions between components and the formation of reaction intermediates, which then react with each other to form the HA structure. Lithium phosphate, Li_3PO_4, is known to have low solubility ($pK_{SP} = 8.5$ [15]), so in reaction (1)

Table 2. Phase composition of the materials

Sample	Phase composition	Percentage		
		900°C	1200°C	1400°C
0Li-HA	$Ca_{10}(PO_4)_6(OH)_2$	100	90	73
	α-$Ca_3(PO_4)_2$	–	–	27
	β-$Ca_3(PO_4)_2$	–	10	–
1Li-HA	$Ca_{10}(PO_4)_6(OH)_2$	100	100	97
	α-$Ca_3(PO_4)_2$	–	–	3
5Li-HA	$Ca_{10}(PO_4)_6(OH)_2$	100	91	85
	β-$Ca_3(PO_4)_2$	–	9	–
	$Ca_{10}Li(PO_4)_7$			15
10Li-HA	$Ca_{10}(PO_4)_6(OH)_2$	100	90	78
	β-$Ca_3(PO_4)_2$	–	10	–
	$Ca_{10}Li(PO_4)_7$		–	22
20Li-HA	$Ca_{10}(PO_4)_6(OH)_2$	100	53	24
	β-$Ca_3(PO_4)_2$	–	20	–
	$LiCaPO_4$	–	27	–
	$Ca_{10}Li(PO_4)_7$	–	–	76

Table 3. Unit-cell parameters and crystallite size (D)

Sample	a, Å (±0.002)	c, Å (±0.002)	D, nm	a, Å (±0.002)	c, Å (±0.002)	D, nm	a, Å (±0.002)	c, Å (±0.002)	D, nm
	900°C			1200°C			1400°C		
0Li-HA	9.420	6.886	58	9.423	6.884	121	9.427	6.910	111
1Li-HA	9.424	6.889	58	9.414	6.881	123	9.423	6.887	83
5Li-HA	9.427	6.879	51	9.419	6.882	117	9.417	6.892	109
10Li-HA	9.425	6.881	59	9.407	6.893	91	9.383	6.869	71
20Li-HA	9.425	6.881	59	A new whitlockite-like phase prevails			A new whitlockite-like phase prevails		

it is most likely to first precipitate. Next, precipitated hydroxyapatite (PHA), having higher solubility (pK_{SP} = ~5.5 in an alkali medium, pH 8.0–8.5 [16]), is formed. Further storage in the mother liquor leads to crystallization of the precipitate, and the PHA reacts with lithium phosphate to form substituted HA materials with better crystallinity in comparison with the parent PHA. Such interaction is possible given that freshly precipitated powders consist of fine particles and exhibit high reactivity. This is confirmed by the present data on the phase composition of powder materials after aging in the mother liquor (Fig. 4), which indicated the presence of a small amount of incompletely reacted compounds—calcium hydroxide and lithium phosphate—in the HA. Note that the formation of lithium phosphate was observed in powders with the highest substituent content.

Thus, we are led to conclude that the final formation of the HA structure and the reaction between HA components reach completion during subsequent high-temperature heat treatments. With allowance for the above, the defect formation reaction for the incorporation of lithium cations into interstices and the formation of an interstitial solution, cation vacancies, and vacancies in the anion sublattice (missing OH groups) can be represented by the following scheme:

$$3Li_3PO_4 \xrightarrow{HA} 9Li_i^{\bullet} + 5V_{Ca}^{''} + V_{OH^-}^{\bullet} + 3PO_{4\,PO_4}^{\times}. \quad (2)$$

Further increasing the amount of lithium ions (5, 10, and 20 mol %) had little effect on the lattice parameters. This can be accounted for in terms of another mechanism of lithium incorporation into the crystal lattice of HA: the formation of substitutional solid solutions, accompanied by the formation of oxygen vacancies:

$$Li_3PO_4 \xrightarrow{HA} 3Li_{Ca}^{'} + V_{PO_4}^{'''} + PO_{4\,PO_4}^{\times}. \quad (3)$$

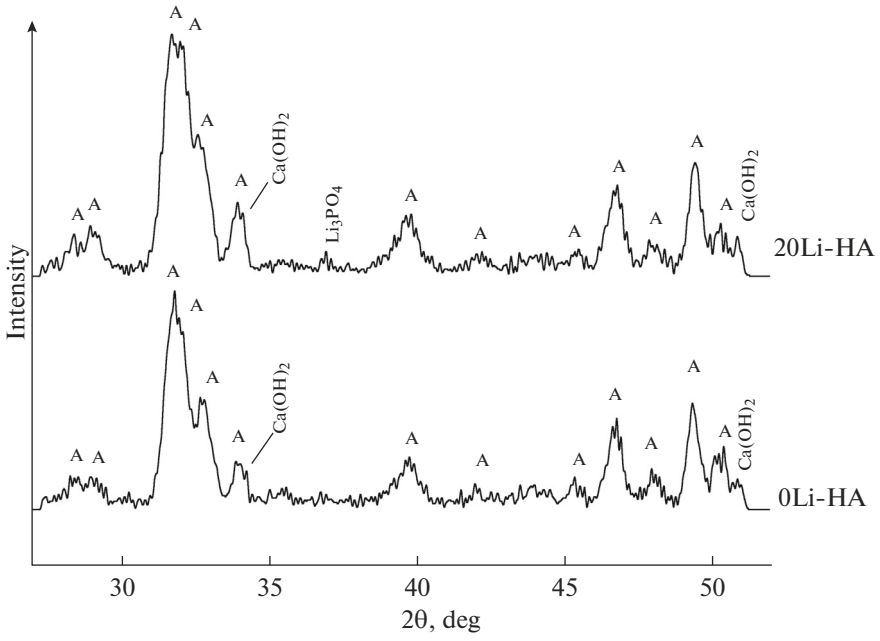

Fig. 4. X-ray diffraction patterns of the powders after aging in the mother liquor.

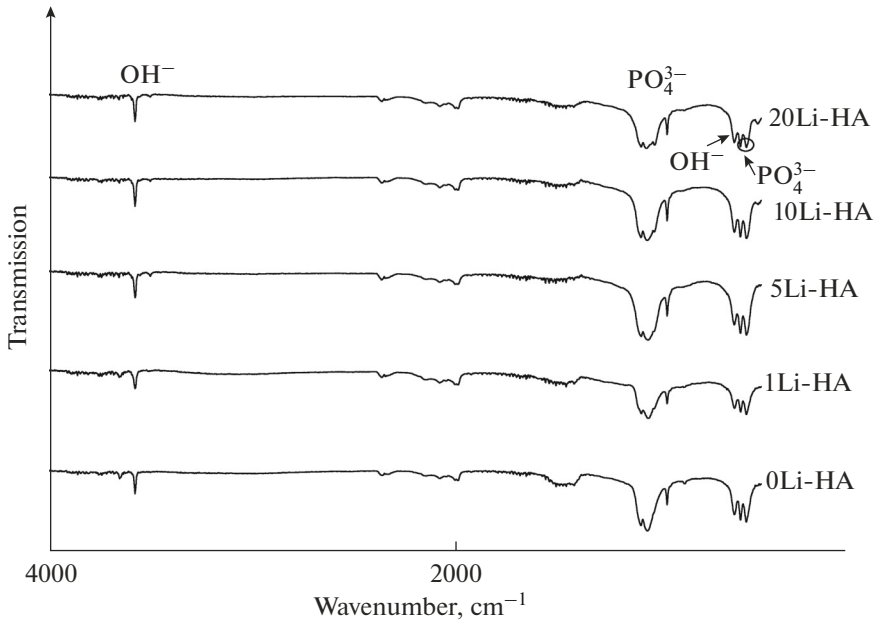

Fig. 5. IR spectra of the samples heat-treated at 900°C.

This reaction scheme also stems from the (calcium + lithium)/phosphorus ratio, which exceeds the calcium/phosphorus ratio in stoichiometric HA. Note that the amount of excess lithium increases with increasing lithium concentration (Table 1). Thus, the forming excess of lithium cations is incorporated into the cation (calcium) sublattice to form vacancies in the anion sublattice (missing PO_4 groups).

Summing up schemes (1) and (2), we obtain a reaction scheme for the formation of solid solutions in the case of materials with a high lithium concentration (5–20 mol %) (reaction (3)). This is accompanied by the formation of both cation and anion vacancies:

$$4Li_3PO_4 \xrightarrow{HA} 9Li_i^{\bullet} + Li_{Ca}^{'} + 5V_{Ca}^{''} + V_{OH}^{\bullet} + V_{PO_4}^{'''} + 4PO_{4\,PO_4}^{\times}. \quad (4)$$

Thus, at low lithium concentrations, the dominant process is the formation of interstitial solid solutions, which leads to an increase in the lattice parameters of the material. Increasing the concentration of lithium cations in HA leads to the formation of interstitial and substitutional solid solutions, and the lattice parameters of the material remain essentially unchanged.

In the case of the materials that had degrees of substitution of 1, 5, and 10 mol % and were heat-treated at 1200 and 1400°C, we observed a tendency toward a decrease in the *a* cell parameter. The *c* cell parameter varied (decreased or increased) little. As pointed out by Belyakov et al. [17], changes in lattice parameters when one of them decreases and another (the other) may increase are typical of the formation of substitutional solid solutions. In the case of the materials with a 20 mol % degree of substitution, the predominantly forming phase is lithium-containing TCP. This is attributable to the thermal instability of lithium-substituted HA as a consequence of the formation of numerous structural defects. This clearly shows up in the case of the 20Li-HA material (Table 1), in which the increasing vacancy concentration (especially the concentration of missing OH groups) contributes to the conversion of HA into TCP [reaction (4)].

IR spectroscopy data demonstrate that the spectra of the samples heat-treated at 900°C are characteristic of HA and differ little from each other (Fig. 5) [18]. Changes in the spectra are observed after heat treatment at a higher temperature of 1200°C. The materials with degrees of substitution from 1 to 5 mol % retain typical vibrations with absorption bands characteristic of phosphate groups (at 573 and 600 cm^{-1} and in the range 960–1188 cm^{-1}) and OH groups (631 and 3571 cm^{-1}) (Fig. 6). As the lithium concentration is raised from 10 to 20 mol %, the 631-cm^{-1} band disappears and the 3571-cm^{-1} band becomes weak. This is due to the loss of water (OH groups) as a result of the conversion of the apatite phase into TCP. After heat treatment at 1400°C, the spectra show no band at 631 cm^{-1}, independent of the degree of substitution. In the spectra of the materials with degrees of substitution of 1, 5, and 10 mol %, the absorption band at 3571 cm^{-1} is weak, whereas in the spectra of the samples containing 0 and 20 mol % lithium this band has negligible intensity (Fig. 7). This indicates that lithium cations stabilize the apatite phase (help the apatite structure to retain hydroxyl groups) at high temperatures (1400°C) and degrees of substitution in the range

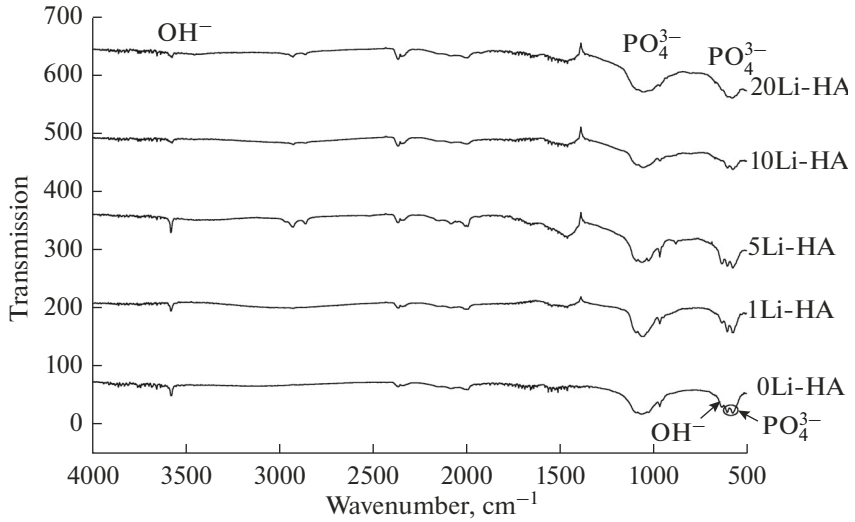

Fig. 6. IR spectra of the samples heat-treated at 1200°C.

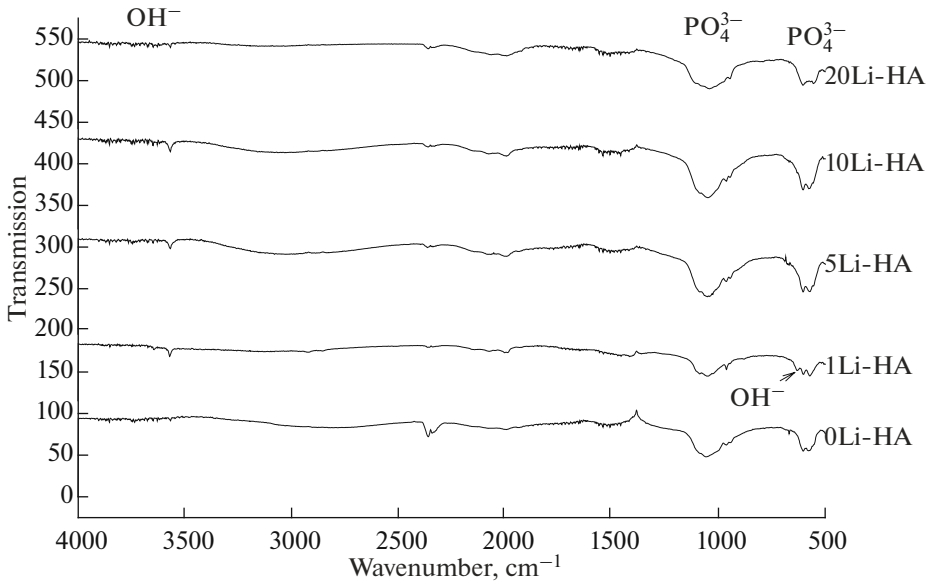

Fig. 7. IR spectra of the samples heat-treated at 1400°C.

1–10 mol %. These conclusions are consistent with the above X-ray diffraction data (Table 2).

The degree of substitution has no marked effect on the crystallite size in the substituted HA materials calcined at 900°C, which range in crystallite size from 47 to 58 nm. At 1200°C, we observe an increase in the crystallite size of the apatite phase in the samples with a relatively low degree of substitution (1 mol %). At the same time, at high lithium concentrations the crystallite size is typically smaller, which is due to the formation of new phases. At a heat treatment temperature of 1400°C, there is a general tendency for the crystallite size to be smaller than that in 0Li-HA. This effect is attributable to the influence of lattice strain. A decrease in lattice parameters is known to be accompanied by a decrease in crystallite size and vice versa: an increase in lattice parameters leads to an increase in crystallite size [12, 17]. Such correlations are especially well-defined in the case of the Li-substituted materials heat-treated at 1400°C: we observe a tendency for their lattice parameters to decrease and, accordingly, a reduction in crystallite size in comparison with HA.

The observed reduction in crystallite size in going from 1200 to 1400°C can be accounted for by the formation of new compounds, which result from a partial transformation of the starting, low-temperature

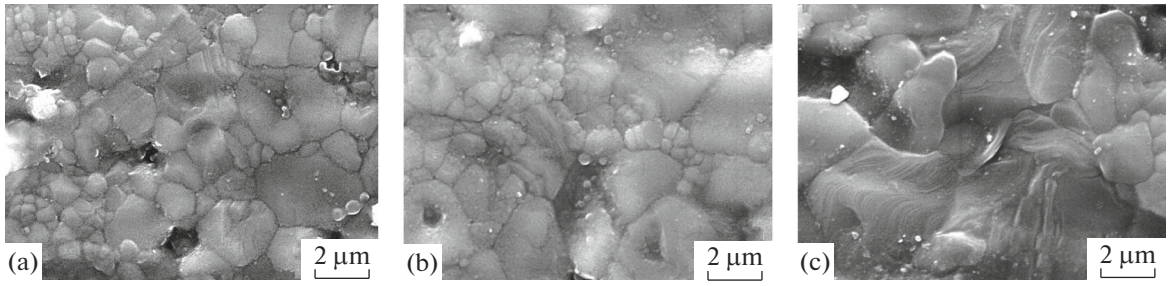

Fig. 8. Microstructures of sintered ceramic materials differing in lithium content: (a) 5Li-HA, (b) 10Li-HA, (c) 20Li-HA.

phases into new, high-temperature, more thermodynamically stable phases. The result is the formation of a few phases instead of one phase (one crystal), which leads to a reduction in crystal size.

Characterization of the samples after sintering (Table 4) showed that the addition of lithium cations helped to obtain dense ceramics. Note that, in the case of the 5Li-HA, 10Li-HA, and 20Li-HA materials, an essentially pore-free state was reached at a temperature as low as 1100°C (Table 4). The decrease in the porosity of the ceramics can be accounted for by the effect of the lithium cations: when embedded in HA, they form both cation and anion defects in the crystal lattice [reactions (2)–(4)], which leads to activation of the solid-state sintering process.

Figure 8 shows microstructures of the materials sintered at 1100°C. It is worth noting that the grain size in the ceramics increases with increasing lithium concentration: the grain size ranges from 0.4 to 4 μm in the 5Li-HA ceramic, from 0.8 to 4 μm in the 10Li-HA ceramic, and from 2 to 5 μm in the 20Li-HA ceramic. In addition, in the structure of the ceramic containing 20 mol % lithium, the grains are more densely packed, which makes grain boundaries poorly discernible. Thus, doping with lithium activates not only the sintering process but also grain growth in the HA ceramics during sintering.

Table 4. Open porosity of the ceramic samples

Temperature, °C	Percent porosity				
	0Li-HA	1Li-HA	5Li-HA	10Li-HA	20Li-HA
1000	55.0	53.3	50.7	20.3	8.8
1100	35.5	12.3	>0.1	>0.1	>0.1
1200	15.5	7.8	>0.1	>0.1	>0.1
1400	>0.1	>0.1	>0.1	>0.1	>0.1

CONCLUSIONS

We have synthesized and investigated a wide range of lithium-substituted powders with the nominal composition of HA. The powders have been heat-treated at 900, 1200, and 1400°C. Lithium cations have been shown to influence the lattice parameters and crystallite size of the materials. It has been shown that, at temperatures of 1200 and 1400°C, lithium cations contribute to a partial conversion of apatite into lithium-substituted TCP phases, whose concentration increases with increasing lithium concentration. At a temperature of 1400°C, lithium cations help the apatite structure to retain OH groups at degrees of substitution of 1, 5, and 10 mol %.

It has been shown that, forming interstitial and/or substitutional solid solutions in HA, depending on the degree of substitution, lithium ions activate the sintering process owing to the formation of both cation and anion vacancies, which makes it possible to obtain dense HA ceramic materials at a temperature as low as 1100°C. The present results should be taken into account in designing the technology of lithium-containing HA ceramics with controlled properties for application in regenerative and reconstructive bone surgery.

FUNDING

This work was supported by the Russian Foundation for Basic Research, grant no. 18-29-11053 mk.

REFERENCES

1. Barinov, S.M., Calcium phosphate-based ceramic and composite materials for medical applications, *Usp. Khim.,* 2010, vol. 79, no. 1, pp. 15–32.
2. Barinov, S.M. and Komlev, V.S., *Biokeramika na osnove fosfatov kal'tsiya* (Calcium Phosphate-Based Bioceramics), Moscow: Nauka, 2005.
3. Kubarev, O.L., Barinov, S.M., and Komlev, V.S., Magnesium distribution in the synthesis of biphasic calcium phosphates, *Dokl. Chem.,* 2008, vol. 418, no. 2, pp. 44–46.
4. Satija, N.K., Sharma, D., Afrin, F., Tripathi, R.P., and Gangenahalli, B., High throughput transcriptome profiling of lithium stimulated human mesenchymal stem

cells reveals priming towards osteoblastic lineage, *PLoS One,* 2013, vol. 8, no. 1, paper e55769.

5. Wang, Y., Yang, X., Gu, Z., Qin, H., Li, L., Liu, J., and Yu, X., In vitro study on the degradation of lithium-doped hydroxyapatite for bone tissue engineering scaffold, *Mater. Sci. Eng., C,* 2016, vol. 66, pp. 185–192.
6. Chen, Y., Whetstone, H.C., Lin, A.C., Nadesan, P., Wei, Q.X., Poon, R., and Alman, B.A., Beta-catenin signaling plays a disparate role in different phases of fracture repair: implications for therapy to improve bone healing, *PLoS Med.,* 2007, vol. 4, pp. 1216–1229.
7. Drdlik, D., Slama, M., Hadraba, H., Drdlikova, K., and Cihlar, J., Physical, mechanical, and biological properties of electrophoretically deposited lithium-doped calcium phosphates, *Ceram. Int.,* 2018, vol. 44, no. 3, pp. 2884–2891.
8. Kaygili, O., Keser, S., Ates, T., and Yakuphanoglu, F., Synthesis and characterization of lithium calcium phosphate ceramics, *Ceram. Int.,* 2013, vol. 39, no. 7, pp. 7779–7785.
9. Badran, H., Yahia, I.S., Hamdy, M.S., and Awwad, N.S., Lithium-doped hydroxyapatite nano-composites: synthesis, characterization, gamma attenuation coefficient and dielectric properties, *Radiat. Phys. Chem.,* 2017, vol. 130, pp. 85–91.
10. Gol'dberg, M.A., Smirnov, V.V., Ievlev, V.M., Barinov, S.M., Kutsev, S.V., Shibaeva, T.V., and Shvorneva, L.I., Influence of ripening time on the properties of hydroxyapatite–calcium carbonate powders, *Inorg. Mater.,* 2012, vol. 48, no. 2, pp. 183–188.
11. Meejoo, S., Maneeprakorn, W., and Winotai, P., Phase and thermal stability of nanocrystalline hydroxyapatite prepared via microwave heating, *Thermochim. Acta,* 2006, vol. 447, no. 1, pp. 115–120.
12. Lukin, E.S., State-of-the-art oxide ceramics with tailored microstructure: Part III. Microstructure and recrystallization processes in ceramic oxide materials, *Ogneupory Tekh. Keram.,* 1996, no. 7, pp. 2–7.
13. Belyakov, A.V. and Lukin, E.S., Physicochemical principles underlying the preparation of powders of solid solutions and mixed oxides, *Tr. Inst.–Mosk. Khim.-Tekhnol. Inst. im. D. I. Mendeleeva,* 1987, no. 146, pp. 5–17.
14. Zhang, X., Mo, F., Zhou, L., and Gong, M., Properties–structure relationship research on $LiCaPO_4$: Eu^{2+} as blue phosphor for NUV LED application, *J. Alloys Compd.,* 2013, vol. 575, pp. 314–318.
15. Efimov, A.I., Belorukova, L.P., Vasil'kova, I.V., and Chechev, V.P., *Svoistva neorganicheskikh soedinenii. Spravochnik* (Properties of Inorganic Compounds: A Handbook), Leningrad: Khimiya, 1983.
16. Chen, Z.F., Darvell, B.W., and Leung, V.W.H., Hydroxyapatite solubility in simple inorganic solutions, *Arch. Oral Biol.,* 2004, vol. 49, no. 5, pp. 359–367.
17. Belyakov, A.V., Lukin, E.S., Popova, N.A., Gorozhenko, Yu.D., Mamaeva, N.B., and Andrianov, N.T., On the sintering of fine powders, *Tr. Inst.–Mosk. Khim.-Tekhnol. Inst. im. D. I. Mendeleeva,* 1988, no. 153, pp. 104–110.
18. Mezahi, F., Oudadesse, H., Harabi, A., Lucas-Girot, A., Le Gal, Y., Chaair, H., and Cathelineau, G., Dissolution kinetic and structural behaviour of natural hydroxyapatite vs. thermal treatment: comparison to synthetic hydroxyapatite, *J. Therm. Anal. Calorim.,* 2008, vol. 95, no. 1, pp. 21–29.

Translated by O. Tsarev